Proceedings of the 3rd International Conference on Modern Medicine and Global Health
DOI: 10.54254/2753-8818/68/2025.18039

Evaluating Retinal Transplantation Success in Degenerated RCS Nude Rats Using Electroretinography

Xia Wu[1,a,*]

[1]*University of California, Irvine, CA, USA*
a. xiaw3@uci.edu
**corresponding author*

Abstract: Our research aims to develop a therapy for incurable retinal diseases, such as retinitis pigmentosa (RP) and age-related macular degeneration (AMD), using the retinal degenerate Royal College of Surgeons (RCS) nude rat model. The approach involves transplanting human embryonic stem cell (hESC)-derived retinal organoid sheets. Photoreceptors in RCS nude rats deteriorate over time, leading to impaired vision, similar to RP and AMD. By transplanting hESC-derived retinal organoid sheets, the degenerated host photoreceptors may be replaced or rescued, potentially halting further degeneration and even enhancing visual performance. Electroretinography (ERG), a noninvasive method, is used to measure visual function. Our current project utilizes ERG to monitor visual responses in RCS nude rats and test whether transplantation of hESC-derived sheets leads to improved light response compared to age-matched control (AMC) non-surgery and sham groups. The left eyes of RCS nude rats were exclusively treated with retinal sheet transplants, allowing for internal comparison. ERG data collected every two months over six months showed a significant decline in visual function with age in both low-light scotopic and bright-light photopic tests for AMC and sham groups. Notably, transplanted RCS nude rats exhibited enhanced responses in the treated left eyes. Together with findings from superior colliculus (SC) recordings and Optokinetic (OKN) assessments, the results suggest that hESC-derived retinal organoid sheets improve visual function in RCS nude rats.

Keywords: Stem cell, macular degeneration, electroretinography.

1. Introduction

Our research focuses on two currently incurable retinal diseases: RP AMD. Retinitis pigmentosa, a hereditary condition, is a leading cause of genetic blindness [1]. Mutations in certain genes cause RP to manifest early in life, making children the most vulnerable. In contrast, AMD primarily affects individuals over fifty and is the most common cause of vision loss among the elderly. In the United States alone, 11 million people are affected by some form of AMD, and this number is expected to double by 2050, making it a widespread disease with no available cure [2]. Both RP and AMD are driven by oxidative stress in the retina and a gradual degeneration of photoreceptors.

The retina is structured with a layer of photoreceptors, crucial for vision, lining the inner side of the eye. Rods, which are sensitive to low light, function best under dim or scotopic conditions, whereas cones, responsible for high light sensitivity and central vision, are tested under brighter, photopic conditions. Rods are primarily located on the outer regions of the retina, while cones

DOI: 10.54254/2753-8818/68/2025.18039

dominate the fovea, an area critical for sharp, central vision. RP is caused by mutations in several genes that lead to the degeneration of both rods and cones. In the early stages of RP, rod deterioration is more common, followed by cone loss in the later stages. Since rods are responsible for vision in dim light, RP patients often experience difficulty seeing in low-light environments. As the disease progresses, patients suffer from deteriorating peripheral vision, eventually leading to tunnel vision. In the advanced stages of RP, when cones start to degenerate, patients face impaired central vision, reduced visual acuity, and difficulty with color perception. The ongoing loss of photoreceptors ultimately results in significant vision loss for RP patients.

AMD patients experience the degeneration of cone photoreceptors, leading to progressive deterioration of the macula, which is responsible for sharp central vision, while peripheral vision remains intact. Current treatments for RP and AMD include daily intake of vitamins and minerals, laser therapy, and anti-angiogenic drugs to address blood vessel leakage in wet AMD [2]. However, despite these methods that can slow or mitigate the progression of retinal diseases, no definitive cure exists for RP or AMD. To explore potential treatments, electroretinography (ERG) is used to track retinal degeneration over time. ERG provides a noninvasive way to measure retinal function by recording responses to light stimuli through scotopic and photopic tests. Phototransduction, the first step in vision, involves photoreceptors converting light into electrical signals, which are then transmitted to the brain via the optic nerve [3]. ERG captures the electrical activity produced, with a focus on analyzing the A-wave and B-wave components of the trace. The A-wave is generated by signals from rod and cone photoreceptors and reflects the outer retinal function before phototransduction. The B-wave, on the other hand, is driven by a transretinal current, originating from inner retinal bipolar cells after phototransduction [4]. Higher amplitudes of these waves indicate better cellular health, with B-waves being particularly important as they reflect the overall retinal condition and are frequently used in both experimental and clinical ERG evaluations [5]. ERG traces, whether scotopic or photopic, provide insight into the visual health of our RCS rat model.

Our goal is to assess the effects of hESC-derived retinal sheet transplants on immunodeficient retinal degeneration in RCS rats using ERG. By analyzing the B-waves, we can evaluate the health of both the photoreceptors and the inner retinal layers. Like human patients with RP and AMD, RCS rats in the age-matched control (AMC) group are expected to show a progressive decline in visual function on their ERG traces. Similarly, the sham group should exhibit comparable visual deterioration. These findings will validate the RCS rat model as a control group for our experimental transplant group, where RCS rats receive hESC-derived retinal sheet transplants. If successful, this approach could pave the way for potential treatments for patients suffering from retinal degeneration.

2. Materials and methods

2.1. Experimental animals

All experiments were carried out in accordance with the Institutional Animal Care and Use Committee at the University of California, Irvine, and were consistent with Federal guidelines. Two to three same-sex rats were housed per cage. The immunodeficient Royal College of Surgeons (RCS) nude rat model, a cross between NIH nude (foxn1-/-) and RCS rats, was utilized. RCS rats carry a mutation in the rhodopsin gene, leading to progressive retinal degeneration. Breeding within the existing immunodeficient RCS colony ensured the retention of immunodeficiency, allowing for successful transplantation of human embryonic stem cells without immune rejection. The rats were assigned to one of three groups: transplant, sham surgery, or age-matched non-surgery controls (AMC).

DOI: 10.54254/2753-8818/68/2025.18039

2.2. Transplantation

The retinal organoids used for transplantation were derived from human embryonic stem cells (hESCs) following a modified protocol based on Zhong et al., 2014 [6]. The hESCs were differentiated in a controlled microenvironment designed to mimic the key stages of retinal development. Retinal organoids, between 30 to 70 days old, were carefully dissected into sheets measuring 0.6 × 1.0 mm and transplanted into the subretinal space of nude RCS rats at around 7 to 8 weeks of age using a custom implantation tool [7]. Sham surgery rats were injected with media only, without any tissue, while AMC rats did not undergo any surgical intervention.

2.3. Electroretinography

ERG testing was typically conducted in groups of 4-7 rats on each testing day. Before the tests, RCS rats were dark-adapted overnight to regenerate rhodopsin, which enhances the sensitivity of rods to light stimuli. Testing was performed under red lighting, and initial anesthesia was induced with 0.5% to 3% isoflurane. Following this, an intraperitoneal injection of 37.5 mg/kg ketamine and 5 mg/kg xylazine in sterile saline was administered to maintain sedation throughout the procedure [0.001x body weight for females, 0.0012x for males]. The rats' whiskers were trimmed to ensure an unobstructed view of the eyes. Equal drops of tetracaine and tropicamide were applied to each eye to numb the muscles and dilate the pupils.

The rats were then positioned on a sliding platform equipped with a heating pad to maintain body temperature. The snout was placed in a plastic mask supplying oxygen and isoflurane if needed, and a temperature probe was inserted rectally. A ground electrode was placed on the lower back, while reference electrodes were positioned on both cheeks. Two recording electrodes, coated with ophthalmic gel to prevent drying and improve conductivity, were placed on the corneas. Once the rat's head was positioned inside the testing dome, the electrodes were calibrated using the ERG machine to ensure stability and minimize noise interference during the recordings.

During testing, the dome emitted light stimuli, which were captured by the recording electrodes. The tests started with scotopic assessments using low-intensity light flashes, followed by more intense photopic tests to stimulate the cones. After testing, Ringer's saline solution [0.1x body weight for both sexes] was administered subcutaneously to maintain hydration. Betadine and antibiotic ointment were applied to the eyes, cheeks, and back to prevent infection. The rats were placed in a recovery chamber and returned to their cages once they regained movement. Data were collected over various time points, ranging from two to six months, and trends in visual function were analyzed and compared across the different groups.

DOI: 10.54254/2753-8818/68/2025.18039

3. Results

3.1. ERG B-wave Traces for the Left Eye at the 2-Month Post-Surgery (2MPS) Time Point with Increasing Flash Intensity

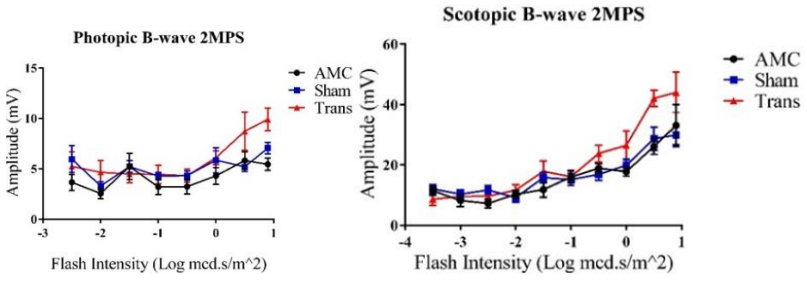

A **B**

Figure 1: Trends show increasing amplitudes represented as Mean ± 1 SEM. A) Average scotopic ERG B-wave amplitudes (mV) in response to increasing flash intensities (Log mcd.s/m^2). Visual responses consistently increased with higher flash intensities. The transplant group demonstrated a significant difference at the highest flash intensity compared to the other groups (N=10). B) Average photopic ERG B-wave amplitudes (mV) with increasing flash intensities (Log mcd.s/m^2). No significant differences were observed between the three groups (N=11).

A t-test was employed to assess the significance and reliability of the collected B-wave amplitudes for all graphs. The null hypothesis was rejected when $P<0.05$ ($\alpha=0.050$). All three groups demonstrated increasing visual responses with higher flash intensities. For graph A), the transplant group exhibited the highest response at the maximum flash intensity compared to the sham group (P=0.046). Although the difference between the transplant and AMC groups was not significant at the highest intensity (P=0.270), there was a notable difference at higher scotopic intensities (P=0.0006 at 0.5 Log mcd.s/m^2). In graph B), significant differences were observed between the transplant and AMC groups (P=0.003) as well as between the transplant and sham groups (P=0.022) at the maximum flash intensity.

3.2. Mean ERG B-wave Traces for the Left Eye at Maximum Flash Intensity

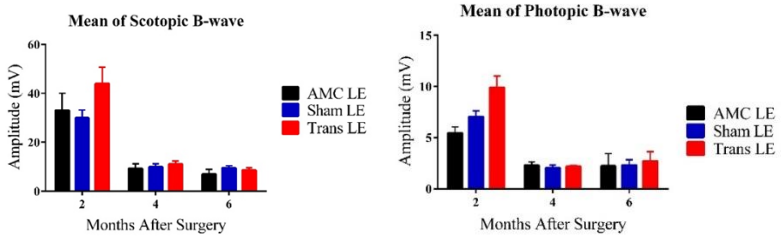

C **D**

Figure 2: Bars represent Mean ± 1 SEM. C) Average scotopic ERG B-wave amplitudes (mV) across age groups (2-6 MPS) for the three experimental groups. At 2MPS: AMC (33.08 ± 6.93 mV), n=10; Sham (29.95 ± 3.24 mV), n=15; Transplant (44.01 ± 6.65 mV), n=10. At 4MPS: AMC (9.29 ± 1.90 mV), n=12; Sham (9.90 ± 1.25 mV), n=12; Transplant (11.02 ± 1.28 mV), n=13. At 6MPS: AMC (6.99 ± 1.91 mV), n=5; Sham (9.50 ± 0.91 mV), n=11; Transplant (8.59 ± 1.00 mV), n=9. D) Average photopic ERG B-wave amplitudes (mV). At 2MPS: AMC (5.45 ± 0.62 mV), n=10; Sham (7.05 ± 0.58 mV), n=15; Transplant (9.90 ± 1.11 mV), n=11. At 4MPS: AMC (2.31 ± 0.32 mV), n=12; Sham (2.04 ± 0.30 mV), n=15; Transplant (2.71 ± 0.94 mV), n=13. At 6MPS: AMC (2.22 ± 1.21 mV), n=4; Sham (2.31 ± 0.52 mV), n=12; Transplant (2.71 ± 0.94 mV), n=9.

DOI: 10.54254/2753-8818/68/2025.18039

At the highest flash intensity, the transplant group showed the strongest scotopic responses (graph C) compared to the AMC and sham groups at 2MPS. The difference between the sham and transplant groups was significant (P=0.046), but no significant difference was observed between the AMC and transplant groups. The responses in the transplant group declined significantly after 2MPS, reaching baseline at 4MPS. Both the AMC and sham groups displayed lower responses at 2MPS, followed by a return to baseline. Once baseline was reached, no significant differences were found among the three groups. In the photopic tests (graph D), the transplant group exhibited significantly higher averages than the AMC (P=0.003) and sham (P=0.022) groups at 2MPS, after which all groups' responses declined to baseline by 4MPS.

3.3. Comparison of Left and Right Eye Responses at Maximum Flash Intensity in the Transplant Group

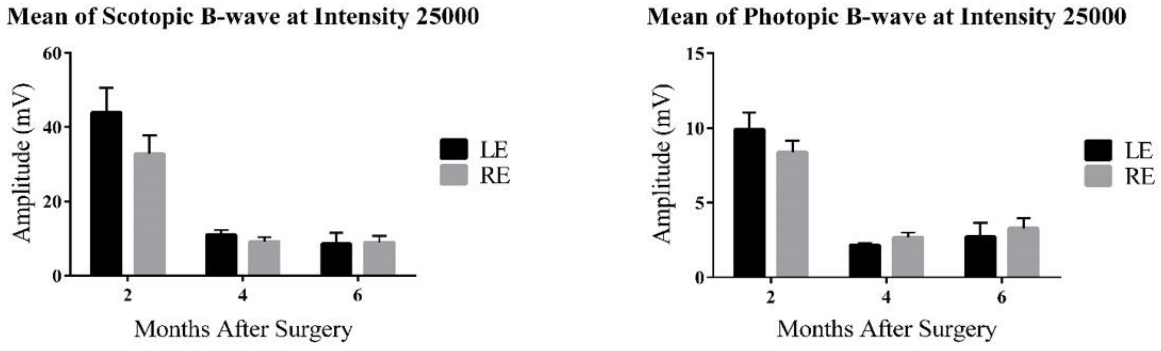

E **F**

Figure 3: Bars represent Mean ± 1 SEM. E) Average scotopic ERG B-wave amplitudes (mV) at the highest flash intensity across age groups (2-6 MPS) for the left and right eyes in the transplant group. F) Average photopic ERG B-wave amplitudes (mV). At 2MPS: n=10; 4MPS: n=13; 6MPS: n=9.

For the scotopic tests (graph E), the left eye exhibited the highest responses at 2MPS, followed by a sharp decline to baseline levels. The average response of the left eye was higher than that of the right eye at 2MPS, but both eyes showed similar response levels by 4MPS and 6MPS. However, the difference between the left and right eyes was not statistically significant (P=0.19). In the photopic tests (graph F), the left eye also showed a higher average response than the right eye, though the difference was not significant (P=0.27). Both eyes reached baseline levels by 4MPS, with no significant differences observed after 2MPS.

4. Discussion

The analysis of ERG results is centered on tracking the progression of B-wave amplitudes, which reflect the health of the inner retina. A degenerated retina, having lost its photoreceptors, produces low B-wave responses, indicating diminished visual function. Conversely, strong B-wave responses suggest the retina retains healthy visual function. In related research investigating treatments for retinal diseases, intravitreal injections of stanniocalcin-1, a protein that reduces oxidative stress—a major factor in AMD and RP—were tested in RCS rats, known for their progressive retinal degeneration. This study yielded positive results, with ERG showing that treated rats exhibited higher scotopic and photopic responses compared to control animals [8].

The data from our experiment supported the hypothesis that RCS nude rats experience retinal degeneration with age. AMC RCS rats displayed a sharp decline in B-wave amplitudes across both

DOI: 10.54254/2753-8818/68/2025.18039

scotopic and photopic tests over the six-month period (Fig. 2). Meanwhile, Figure 1 demonstrated that visual responses increased with rising flash intensity across all groups. Given that the most significant differences in scotopic and photopic amplitudes occurred at the maximum flash intensity, B-wave amplitudes at this intensity were compared across groups at three different time points. By 2MPS, the retinal function of the degenerating RCS rats had reached baseline levels, making it difficult to precisely measure the remaining function of the degenerated retina. This likely explains the variability in the trends observed after 2MPS. The sham group displayed similar trends, having only received media injections (Fig. 2). The significant difference between the transplant and sham groups at 2MPS suggests that hESC-derived retinal organoids were successful in rescuing residual photoreceptors. The lack of significant difference between the AMC and transplant groups at 2MPS could be attributed to the small sample size and potential noise in the ERG measurements. In a previous study by Seiler et al. [7], no significant improvement in vision was detected in ERG tests, likely because the transplanted sheet covered a relatively small area of the retina. B-wave amplitudes across all groups dropped to baseline at 4MPS and became undetectable thereafter. While the differences were not statistically significant at 2MPS, the transplant group still showed higher average responses. Scotopic responses in the transplant group were higher at 2MPS, followed by a sharp decline (Fig. 2, C). As B-wave amplitudes approached baseline, they began to resemble those of the AMC and sham groups. Like Seiler et al.'s findings, the limited size of the transplanted area may explain the decline [7]. Other potential reasons for the lack of statistical significance include the small sample sizes (around 10 individuals per group at each time point) and potential noise in the ERG measurements, which could have led to higher standard errors. For the photopic tests (Fig. 2, D), the amplitudes were small, and the differences were within the standard error (~5 mV). Since all groups' amplitudes had dropped to baseline, the differences between the transplant and other groups were not statistically significant.

Within the transplant group (Fig. 3, E), the left eyes exhibited higher scotopic responses than the right eyes at 2MPS, although the difference was not statistically significant. This could be attributed to the small sample size and potential noise captured by the ERG machine. According to studies by Sauvé et al., left eyes receiving transplants tend to show stronger responses shortly after surgery. However, the reliability of our results must be further validated by conducting additional ERG tests on RCS transplant rats. For the photopic tests, while the left eyes showed slightly higher responses than the right eyes, the small scale of detected responses made it difficult to determine significance. As with the scotopic tests, additional ERG testing is required to confirm the reliability of these results. The ERG tests indicated that photoreceptors in RCS rats with degenerative retinal disease gradually deteriorated with age, leading to weakened retinal responses, especially to photopic stimuli. RCS rats that received hESC-derived retinal organoids exhibited higher visual responses to light stimuli in the early stages after surgery, with responses declining to baseline levels by 4MPS.

Looking ahead, our group plans to continue ERG testing at 2, 4, and 6 MPS to reduce standard errors for each group and improve the reliability of the results. Additionally, we will expand the testing schedule to include more time points: 1 and 2 weeks before surgery, as well as 1, 3, and 5 MPS. Incorporating ERG data from all time points will enable us to track visual changes over time and better assess the success of hESC-derived retinal organoids. By combining these findings with other experimental data, such as superior colliculus (SC) recordings, optical coherence tomography (OCT) scans, and optokinetic testing (OKT), we can more accurately determine the effectiveness of hESC-derived sheet transplants in improving vision in immunodeficient retinal degenerate RCS rats. This will pave the way for future transplantation trials in other retinal degeneration models, representing significant progress toward clinical trials and advancing treatments for currently incurable retinal degenerative diseases like AMD and RP.

DOI: 10.54254/2753-8818/68/2025.18039

5. Conclusion

Our study demonstrates that hESC-derived retinal organoid transplantation can temporarily improve visual function in immunodeficient retinal degenerate RCS rats, as shown by enhanced scotopic and photopic responses shortly after surgery. However, these improvements gradually decline to baseline levels by 4MPS, indicating the need for further optimization of transplantation techniques and long-term effectiveness. The data support the potential of stem cell-based therapies to rescue degenerated photoreceptors, offering hope for future treatments of retinal degenerative diseases such as AMD and RP. Ultimately, these steps bring us closer to developing viable clinical treatments for currently incurable retinal conditions.

References

[1] *Huang, X. F., Wu, J., Lv, J. N., Zhang, X., & Jin, Z. B. (2015). Identification of false-negative mutations missed by next-generation sequencing in retinitis pigmentosa patients: a complementary approach to clinical genetic diagnostic testing. Genetics in Medicine, 17(4), 307-311.*

[2] *Curcio, C. A., Medeiros, N. E., & Millican, C. L. (1996). Photoreceptor loss in age-related macular degeneration. Investigative ophthalmology & visual science, 37(7), 1236–1249.*

[3] *Kolb, H. (2003). How the retina works: Much of the construction of an image takes place in the retina itself through the use of specialized neural circuits. American scientist, 91(1), 28-35.*

[4] *Bhatt, D. (2013). Electrophysiology for ophthalmologist (A practical approach). Journal of Clinical Ophthalmology and Research, 1(1), 45-53.*

[5] *Asi, H., & Perlman, I. (1992). Relationships between the electroretinogram a-wave, b-wave and oscillatory potentials and their application to clinical diagnosis. Documenta Ophthalmologica, 79, 125-139.*

[6] *Zhong, X., Gutierrez, C., Xue, T., Hampton, C., Vergara, M. N., Cao, L. H., ... & Canto-Soler, M. V. (2014). Generation of three-dimensional retinal tissue with functional photoreceptors from human iPSCs. Nature communications, 5(1), 4047.*

[7] *Seiler, M. J., Lin, R. E., McLelland, B. T., Mathur, A., Lin, B., Sigman, J., ... & Thomas, B. B. (2017). Vision recovery and connectivity by fetal retinal sheet transplantation in an immunodeficient retinal degenerate rat model. Investigative ophthalmology & visual science, 58(1), 614-630.*

[8] *Roddy, G. W., Rosa Jr, R. H., Oh, J. Y., Ylostalo, J. H., Bartosh, T. J., Choi, H., ... & Prockop, D. J. (2012). Stanniocalcin-1 rescued photoreceptor degeneration in two rat models of inherited retinal degeneration. Molecular Therapy, 20(4), 788-797.*